

Energy Gap of the Even-Denominator Fractional Quantum Hall State in Bilayer Graphene

Alexandre Assouline¹, Taige Wang,^{2,3} Haoxin Zhou¹, Liam A. Cohen¹, Fangyuan Yang,¹ Ruining Zhang,¹ Takashi Taniguchi,⁴ Kenji Watanabe⁵, Roger S. K. Mong,⁶ Michael P. Zaletel,^{2,3} and Andrea F. Young^{1,*}

¹*Department of Physics, University of California at Santa Barbara, Santa Barbara, California 93106, USA*


²*Department of Physics, University of California, Berkeley, California 94720, USA*

³*Material Science Division, Lawrence Berkeley National Laboratory, Berkeley, California 94720, USA*

⁴*International Center for Materials Nanoarchitectonics, National Institute for Materials Science, 1-1 Namiki, Tsukuba 305-0044, Japan*

⁵*Research Center for Functional Materials, National Institute for Materials Science, 1-1 Namiki, Tsukuba 305-0044, Japan*

⁶*Department of Physics and Astronomy, University of Pittsburgh, Pittsburgh, Pennsylvania 15260, USA*

 (Received 28 July 2023; revised 10 December 2023; accepted 4 January 2024; published 26 January 2024)

Bernal bilayer graphene hosts even-denominator fractional quantum Hall states thought to be described by a Pfaffian wave function with non-Abelian quasiparticle excitations. Here, we report the quantitative determination of fractional quantum Hall energy gaps in bilayer graphene using both thermally activated transport and by direct measurement of the chemical potential. We find a transport activation gap of 5.1 K at $B = 12$ T for a half filled $N = 1$ Landau level, consistent with density matrix renormalization group calculations for the Pfaffian state. However, the measured thermodynamic gap of 11.6 K is smaller than theoretical expectations for the clean limit by approximately a factor of 2. We analyze the chemical potential data near fractional filling within a simplified model of a Wigner crystal of fractional quasiparticles with long-wavelength disorder, explaining this discrepancy. Our results quantitatively establish bilayer graphene as a robust platform for probing the non-Abelian anyons expected to arise as the elementary excitations of the even-denominator state.

DOI: [10.1103/PhysRevLett.132.046603](https://doi.org/10.1103/PhysRevLett.132.046603)

Non-Abelian anyons [1] are thought to enable fault-tolerant topological quantum bits through their nontrivial braiding statistics [2,3]. In an ideal scenario, the error rate of such qubits is limited only by the density of thermally excited quasiparticles present in the system. Such processes— analogous to quasiparticle poisoning in superconducting qubits—are exponentially suppressed at low temperature by an Arrhenius law, $n_{qp} \propto \exp(-\Delta_{qp}/2k_B T)$, where Δ_{qp} is the energy gap for non-Abelian quasiparticles and T is the temperature. The energy gap is, thus, a key figure of merit for candidate non-Abelian states. According to numerical calculations [4,5], non-Abelian ground states are the leading candidates to describe the even-denominator fractional quantum Hall (FQH) states observed in the second orbital Landau level of single-component systems such as GaAs quantum wells [6]. While these numerical results are thought to be reliable, the small energy gaps measured for these states in GaAs [7–10] have hampered experimental efforts to directly probe non-Abelian statistics via fusion and braiding of individual quasiparticles.

Within the simplest model of bilayer graphene, the $N = 0$ and $N = 1$ orbital levels are both pinned to zero energy [11]. Combined with the spin and valley degeneracies native to graphene quantum Hall systems [12], this produces an eightfold degeneracy—a seemingly inauspicious arena for the single-component physics of

non-Abelian FQH states. However, as a wealth of experimental work has shown, all of these degeneracies are lifted by the combination of electronic interactions and the applied displacement field [13–23]. In particular, broad domains of density and displacement field are characterized by partial filling of a singly degenerate $N = 0$ or $N = 1$ Landau level. In the $N = 1$ regime, an incompressible state is observed at half-integer filling [18,21–23], which calculations show should be described by a non-Abelian Pfaffian ground state [22,24–26]. Prior measurements of energy gaps have found activation gaps as large as 1.8 K at $B = 14$ T; however, precise comparisons of activation and thermodynamic gaps to theoretical expectations have not been previously reported.

Here, we report energy gaps for both odd- and even-denominator FQH states in bilayer graphene using both transport and chemical potential measurements. Thermally activated transport measures the energy cost of creating a physically separated quasiparticle-quasihole pair. We measure activated transport using a Corbino-like geometry [27,28], which directly probes the conductivity of the gapped, insulating bulk. Chemical potential measurements record a jump at incompressible filling factors known as the thermodynamic gap, which—in the clean limit—measures the difference between adding charge $\pm e$ to the gapped system. We measure the thermodynamic gap using a direct-current charge sensing technique based on a

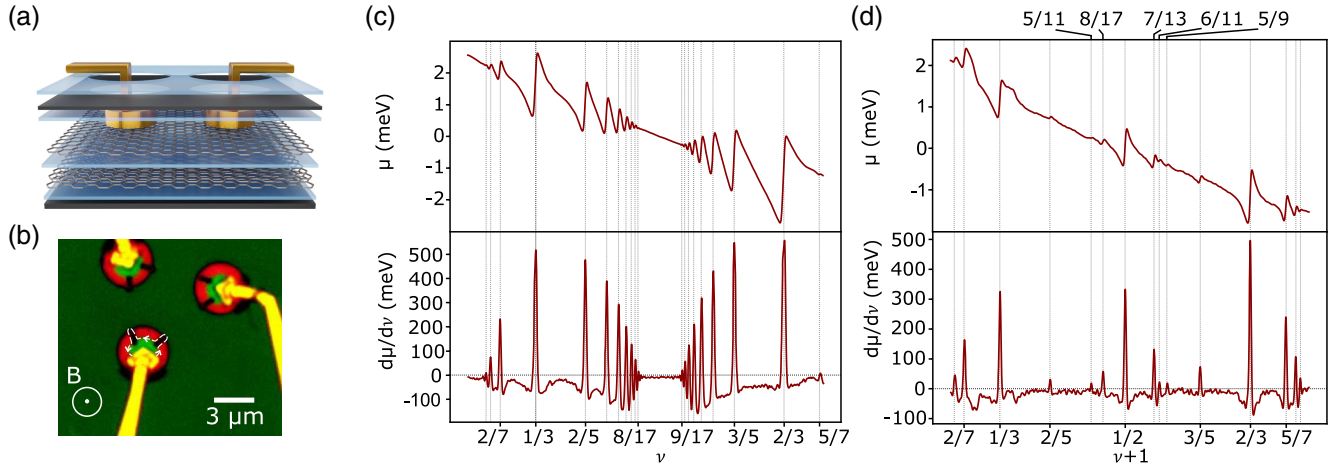


FIG. 1. Chemical potential and inverse compressibility of bilayer graphene fractional quantum Hall states. (a) Device schematic showing the h -BN layers (blue), top and bottom graphite gates (dark gray), monolayer graphene detector layer connected to Corbino contacts, and bilayer graphene sample layer. (b) Optical image of the Corbino contacts to the monolayer graphene detector. White dashed lines show the trajectory of a chiral edge state along trenches etched through the device, which ensures contact between the metal and dual-gated sample bulk. (c) The top panel shows the measured μ at $B = 13.8$ T and $T = 50$ mK in the partially filled $N = 0$ level spanning $0 < \nu < 1$. The bottom panel shows the inverse compressibility $d\mu/d\nu$, calculated by numerically differentiating the data in the top panel. (d) The same as (c) but for the partially filled $N = 1$ orbital Landau level spanning $-1 < \nu < 0$.

double-layer device [29,30]. Combining these techniques, we find several new features, including weak FQH states at $\nu = 5/11$, $\nu = 6/11$, and $\nu = 5/9$ of a partially filled $N = 1$ Landau level. Moreover, both schemes show an energy gap for a half filled single-component Landau level that is several times larger than reported to date for a candidate non-Abelian state in any system [7–9,22,23,31–33]. Notably, these measurement schemes effectively average over $\sim 10 \mu\text{m}^2$ -sized areas, a testament to the exceptional uniformity of the electron gas in bilayer graphene.

Figure 1(a) shows a schematic of the experimental geometry used to measure the chemical potential μ . A graphene bilayer hosting the FQH system of interest is separated by a 62-nm-thick hexagonal boron nitride (h -BN) dielectric from a graphene monolayer that functions as a sensor. Both layers are encapsulated by additional h -BN dielectrics and graphite gates, creating a four-plate geometry that allows independent control of the carrier density on both the monolayer detector and bilayer sample layer. We measure Corbino transport in the detector layer, where a FQH state functions as a sensitive detector of the local potential. An optical image of the Corbino contacts is shown in Fig. 1(b). As described in detail in Supplemental Material [34], monitoring transport in the sensor layer allows us to precisely determine μ of the bilayer sample. An advantage of our technique is that it avoids finite-frequency modulation of the carrier density, allowing us to accommodate charge equilibration times as large as a second. The current technique is less invasive than previous capacitance measurements [22], requiring no modulation of the sample density and reducing heating due to cryogenic semiconductor amplifiers.

Figures 1(c) and 1(d) show μ and $d\mu/d\nu$ measured in our bilayer graphene device at $B = 13.8$ T. In the $N = 0$ Landau level, incompressible spikes are observed at fillings corresponding to the two- and four-flux “Jain” sequence [39], with denominators as high as 17. In the $N = 1$ orbital, a different hierarchy is observed, including a prominent state at $\nu + 1 = 1/2$ along with states at $8/17$ and $7/13$ filling. This sequence is consistent with a Pfaffian state at half filling and Abelian “daughter” states built from its elementary excitations [22,40]. Additional peaks are observed at fillings consistent with the four-flux Jain sequence, at $3/5$ and $2/5$, and finally several weaker states at $5/11$, $6/11$, and $5/9$ which were not previously reported. Away from these incompressible fillings, the compressibility is negative throughout the partially filled Landau level [41,42]. Additional negative compressibility is observed near the incompressible states, associated with the formation of Wigner crystals of fractionally charged quasiparticles at low quasiparticle density.

Figure 2(a) shows the two-terminal conductance (G) in a second sample consisting of a dual-gated bilayer with Corbino-like geometry (see Supplemental Material [34]). Measurements are taken at $B = 12$ T in a partially filled $N = 1$ Landau level corresponding to filling factors $0.25 \lesssim \nu + 3 < 0.75$ (see Supplemental Material [34]). The activation gap and chemical potential measurements were not performed in the same filling factor range due to constraints arising from the electrical contacts to the bilayer or sensor layer. However, the states originate from the same orbital level and differ only in their valley isospin. Consequently, they are treated theoretically in the same way, taking into account orbital levels and a single spin or valley

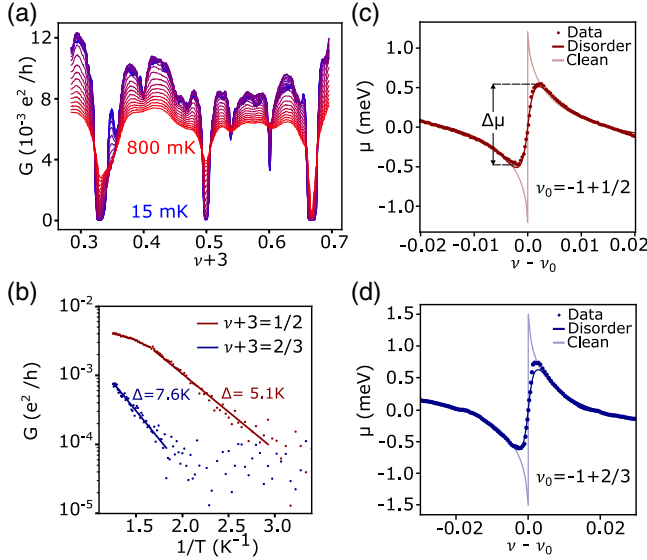


FIG. 2. Comparison of activation and thermodynamic gaps in a partially filled $N = 1$ Landau level. (a) Two-terminal conductance measured in a Corbino geometry as a function of filling factor at $B = 12$ T for different temperatures. The temperature spacing is 5 mK. (b) Activation gap from the Arrhenius fit for $\nu = -3 + 1/2$ (red) and $\nu = -3 + 2/3$ (blue). (c) Chemical potential measurement near $\nu_0 = -1 + 1/2$ (red dots) at $B = 13.8$ T. Theory fit using the Wigner crystal model in the clean limit (light red line) and in the disordered limit (red line). (d) Chemical potential measurement near $\nu_0 = -1 + 2/3$ (blue dots) at $B = 13.8$ T. Theory fit using the Wigner crystal model in the clean limit (light blue line) and in the disordered limit (blue line).

component. The three most prominent FQH states, at $\nu + 3 = 1/3, 1/2$, and $2/3$, all show vanishing conductance at the lowest temperatures. Figure 2(b) shows the minimal conductance for $\nu + 3 = 1/2$ and $2/3$ as a function of the temperature, along with fits to an Arrhenius law $G \propto n_{\text{qp}} \propto e^{-\Delta_{\text{qp}}/2k_B T}$. For the $1/2$ state, the activation gap is found to be 5.1 K at $B = 12$ T, considerably larger than previous measurements in other two-dimensional electron systems [7–10,32,33]. The increase relative to the GaAs $\nu = 5/2$ state is expected due to the higher electron density and lower dielectric constant of the van der Waals platform. Interestingly, the gap is also much larger than previously reported in bilayer graphene [22,23], under the same conditions. We attribute this to the Corbino geometry used here, which directly probes the bulk conductivity, avoiding systematic underestimates resulting from poor equilibration of electrical contacts with the chiral edge states [27,28].

We may compare the result for the activation gap with a numerical calculation that accounts for the microscopic details of bilayer graphene, accomplished using the density matrix renormalization group (DMRG) [43,44]. Following Ref. [22], these calculations are conducted on an infinite

cylinder within a four-band model of bilayer graphene and account for mixing between the $N = 0$ and 1 Landau levels, screening from the gates and—crucially—screening due to inter-Landau level transitions, which is treated within the random phase approximation (see Supplemental Material [34]). We obtain a quasiparticle gap $\Delta_{\text{qp}}^{\text{DMRG}} = 0.011E_C$, where the Coulomb energy scale E_C depends on both the magnetic field and the dielectric constant for h -BN, which we take as $\epsilon_{h\text{-BN}} = \sqrt{\epsilon_{xy}\epsilon_z} = 4.5$ [30]. The calculated gap is 5.6 K at 12 T, within 10% of the experimental value.

The jump in chemical potential at fractional filling, $\Delta\mu$, provides an alternative measurement of the FQH energy gaps, as shown in Figs. 2(c) and 2(d) measured at $B = 13.8$ T. For the $1/2$ state in Fig. 2(c), the $\Delta\mu$ jump of 1.0 meV corresponds to a temperature of 11.6 K. In the clean limit, $\Delta\mu$ corresponds to the energy cost of adding a whole electron to the gapped system and is expected to be e/e^* times larger than the quasiparticle gap, where e^* is the quasiparticle charge. At $\nu = -1/2$, where $e/e^* = 4$, the quasiparticle gap $\Delta_{\text{qp}}^\mu = \Delta\mu/4 = 2.9$ K implied by the thermodynamic measurement is significantly smaller than $\Delta_{\text{qp}}^{\text{act}} \approx 5.1$ K, even before accounting for the small difference in B between Figs. 2(a) and 2(c). A similar discrepancy is seen at $\nu + 1 = 2/3$, where $\Delta_{\text{qp}}^{\text{act}} \approx (7.6 \pm 0.5)$ K but the quasiparticle gap from thermodynamic measurements is $\Delta_{\text{qp}}^\mu = 5.2$ K.

We attribute the discrepancy to the contrasting role of disorder on the thermodynamic and activation gaps. In the simplest model for activated transport [45], disorder does not reduce the activation gap, while in more detailed models the activation gap is reduced by an amount that depends on the spatial correlations of the disorder potential [46,47]. On the other hand, disorder always reduces the thermodynamic gap, as it produces in-gap localized states which result in a finite compressibility. So, while disorder affects both gaps, it does so through different mechanisms, and we expect the reduction of the thermodynamic gap to be larger. To assess this hypothesis, we compare our data against a phenomenological model for $\mu(\nu)$ that accounts for both the disorder and quasiparticle interactions. Our model assumes that the compressible states adjacent to the incompressible FQH states are Wigner crystals of fractionally charged quasiparticles [42,48]. As a starting point, we compute the energy density $\mathcal{E}(\nu)$ of this pristine Wigner crystal under the assumption that the fractional point charges e^* form a triangular lattice and interact through an effective Coulomb potential which accounts for screening from the gates as well as the dielectric response of the parent gapped state. In the disorder-free limit, we obtain theoretical $\mu(\nu)$ curves in which an infinitely sharp jump of $\Delta\mu = (e/e^*)\Delta_{\text{qp}}^\mu$ is flanked by the negative compressibility of the screened Wigner crystal (see Supplemental Material [34]). As shown in Figs. 2(c) and 2(d), we find this disorder-free model provides a good fit to the data at

TABLE I. Comparison of the quasiparticle gaps at $1/2$ and $2/3$ filling in the $N = 1$ Landau level as determined by DMRG calculations $\Delta_{\text{qp}}^{\text{DMRG}}$, thermally activated transport $\Delta_{\text{qp}}^{\text{act}}$, the chemical potential jump Δ_{qp}^{μ} , and from the fit to the Wigner crystal model $\Delta_{\text{qp}}^{\text{fit}}$.

Filling $\nu + 1$	B	$\Delta_{\text{qp}}^{\text{act}}$	Δ_{qp}^{μ}	$\Delta_{\text{qp}}^{\text{fit}}$	$\Delta_{\text{qp}}^{\text{DMRG}}$
$\frac{1}{2}$	12 T	5.1 K	5.6 K
	13.8 T	...	2.9 K	7.0 K	6.0 K
$\frac{2}{3}$	12 T	7.6 K	10.8 K
	13.8 T	...	5.2 K	11.6 K	11.7 K

moderate quasiparticle densities, where the compressibility is strongly negative.

To account for disorder, we make the assumption that the disorder potential varies slowly in comparison with both the interquasiparticle distance and the distance to the gates. As described in Supplemental Material [34], this allows us to make a local density approximation; $\mu(\nu)$ can then be solved for explicitly given the interaction energy density $\mathcal{E}(\nu)$ and the disorder distribution $P[V_D]$, which we assume to be a Gaussian of width Γ . We note that these assumptions may not be correct. For example, it will not be the case if the disorder arises from dilute Poisson-distributed charge impurities in the h -BN. Nevertheless, it results in a tractable model that accounts for the competition between disorder and interactions.

Fits to this model are shown in Figs. 2(c) and 2(d) near $\nu = -1 + 1/2$ and $\nu = -1 + 2/3$. The fit is parametrized by the quasiparticle gap $\Delta_{\text{qp}}^{\text{fit}}$, a phenomenological parameter χ which accounts for the dielectric response of the parent state, and the disorder broadening Γ (see Supplemental Material [34]). We find quantitative agreement between the Wigner crystal model and experiment, providing strong evidence for a Wigner crystal of fractionalized quasiparticles. From the fit, we infer $\Delta_{\text{qp}}^{\text{fit}} = 7$ K for the $1/2$ state, within 20% of $\Delta_{\text{qp}}^{\text{DMRG}} = 6.0$ K. The same analysis for the $\nu_0 = -1 + 2/3$ gives $\Delta_{\text{qp}}^{\text{fit}} = 11.6$ K, again within 20% of the $\Delta_{\text{qp}}^{\text{DMRG}} = 11.7$ K. For both fillings, we find $\Gamma = 1.0 \pm 0.5$ meV, consistent with previous estimates for the Landau level broadening [27,28]. The comparison between experimental and theoretical gaps is summarized in Table I.

Given the rather large discrepancies between experiment and numerics in GaAs [49]—particularly at half filling—the level of agreement we find for both activated and thermodynamic gaps with numerical modeling is encouraging. We note that several sources may account for the remaining quantitative discrepancies in our work. These include differences in inter-Landau level screening strength at $\nu \sim -3$ relative to $\nu \sim -1$ [50], as well as possible spin textures in the excitation spectrum, which can lower the activation gap but are not accounted for in

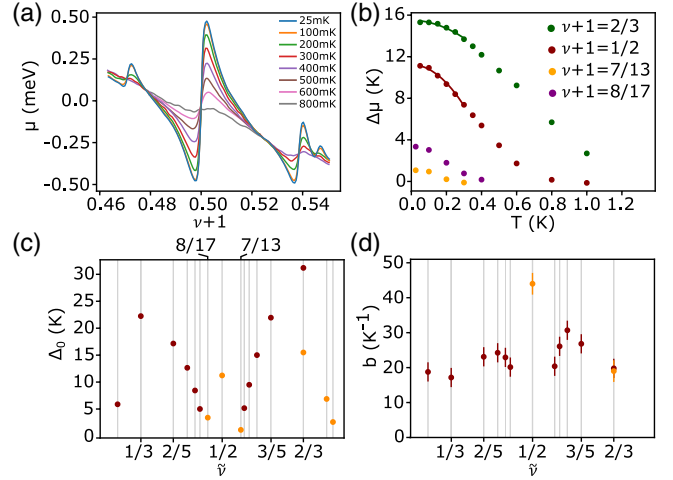


FIG. 3. Temperature-dependent μ near fractional filling. Measurements are performed at $B = 13.8$ T. (a) Chemical potential near half filling of an $N = 1$ Landau level at several different temperatures. (b) Chemical potential jump across the incompressible states as a function of the temperature for different filling factors in an $N = 1$ LL (dots). The solid lines are a low-temperature fit, $\Delta\mu(T) = \Delta_0 - bT^2$. (c) Chemical potential jump Δ_0 extracted from the fit for different fractional states in the $N = 0$ ($\tilde{\nu} = \nu$, red dots) and $N = 1$ ($\tilde{\nu} = \nu + 1$, orange dots) orbital Landau levels. (d) Temperature decay parameter b extracted from the fit.

our modeling. For $\Delta_{\text{qp}}^{\text{fit}}$, moreover, the phenomenological nature of our model for disorder may not capture the microscopic physics at a quantitative level. Finally, we note that the discrepancy between theory and experiment is greater at $2/3$ than at $1/2$, perhaps due to the greater quasiparticle charge resulting in a greater effect of the disorder potential.

Figure 3(a) shows the μ measured at different temperatures near the $\nu + 1 = 1/2$ gap. We focus on the strong temperature dependence of $\Delta\mu$, plotted for several incompressible filling factors in Fig. 3(b) (see also Supplemental Material [34]). We fit the low-temperature limit of $\Delta\mu(T)$ using the Sommerfeld expansion $\Delta\mu(T) = \Delta_0 - bT^2 + \dots$, which is justified so long as the quasiparticles experience short-range repulsion. The fitted values Δ_0 and b are reported in Figs. 3(c) and 3(d), respectively.

Notably, the $\nu = -1 + 1/2$ state shows anomalously strong temperature dependence, manifesting as a large value of the b parameter. Note that this state becomes compressible at about 800 mK in Fig. 3(a), which corroborates with the deviation from activated transport at high temperature in Fig. 2(b). According to the Maxwell relation $(d\mu/dT)|_n = -(ds/dn)|_T$, this suggests an anomalous contribution to the entropy in the dilute quasiparticle limit. Anomalous entropy is expected in the vicinity of non-Abelian states [51] owing to the topological degeneracy of a dilute gas of non-Abelian anyons. However, this contribution is considerably smaller than the anomalous

entropy we observe. This implies that the anomalous entropy near $\nu = 1/2$ —at least at the filling factors corresponding to the extrema in μ —does not arise solely from the topological degeneracy. Notably, these extrema occur at a density of quasiparticles where the average interquasiparticle distance is larger than the distance to the gate. Disorder is expected to dominate this regime, as interquasiparticle interactions are screened. Crudely, if disorder is more important than the long-range Coulomb interaction, we expect $b \propto (e/e^*)^2/\Gamma$, where Γ is the strength of the disorder. However, determining the prefactor requires understanding the thermodynamics of a Coulomb glass of fractionalized particles in an unknown disorder distribution, a challenge we leave to future work.

In closing, we note that a related manuscript reports scanning tunneling microscopy to study the same bilayer graphene FQH states studied here [52]. In that work, the gate voltage δV_g over which the FQH gaps appear provides a local measurement of the thermodynamic gap. Those authors find $4\Delta_{\text{qp}}^{\text{STM}} = 30$ K for the $1/2$ state at $B = 14$ T. This result is consistent with the intrinsic gap inferred from our Wigner crystal (WC) model, $4\Delta_{\text{qp}}^{\text{WC}} \sim 28$ K, as expected for a local measurement that probes the chemical potential at length scales smaller than the disorder correlation length. The large intrinsic gaps manifesting across several experimental techniques show that bilayer graphene is an ideal platform to explore the intrinsic physics of non-Abelian anyons in the solid state.

The authors acknowledge discussions with A. Stern, A. Yazdani for a related collaboration and sharing unpublished results, and E. Redekop for providing the device image shown in Fig. 1(a). Experimental work at UCSB was primarily supported by the Office of Naval Research under Grant No. N00014-23-1-2066 to A. F. Y. A. F. Y. acknowledges additional support by Gordon and Betty Moore Foundation EPIQS program under Grant No. GBMF9471. M. P. Z. and T. W. were supported by the U.S. Department of Energy, Office of Science, Office of Basic Energy Sciences, Materials Sciences and Engineering Division, under Contract No. DE-AC02-05CH11231, within the van der Waals Heterostructures Program (KCWF16). R. S. K. M. is supported by the National Science Foundation under Grant No. DMR-1848336. K. W. and T. T. acknowledge support from the Elemental Strategy Initiative conducted by the MEXT, Japan (Grant No. JPMXP0112101001) and JSPS KAKENHI (Grants No. 19H05790, No. 20H00354, and No. 21H05233). This research used the Lawrence computational cluster provided by the Lawrence Berkeley National Laboratory (supported by the U.S. Department of Energy, Office of Basic Energy Sciences under Contract No. DE-AC02-05CH11231).

*andrea@physics.ucsb.edu

- [1] G. Moore and N. Read, *Nucl. Phys.* **B360**, 362 (1991).
- [2] A. Y. Kitaev, *Ann. Phys. (Amsterdam)* **303**, 2 (2003).
- [3] C. Nayak, S. H. Simon, A. Stern, M. Freedman, and S. Das Sarma, *Rev. Mod. Phys.* **80**, 1083 (2008).
- [4] R. H. Morf, *Phys. Rev. Lett.* **80**, 1505 (1998).
- [5] E. H. Rezayi, *Phys. Rev. Lett.* **119**, 026801 (2017).
- [6] R. Willett, J. P. Eisenstein, H. L. Stormer, D. C. Tsui, A. C. Gossard, and J. H. English, *Phys. Rev. Lett.* **59**, 1776 (1987).
- [7] A. Kumar, G. A. Csáthy, M. J. Manfra, L. N. Pfeiffer, and K. W. West, *Phys. Rev. Lett.* **105**, 246808 (2010).
- [8] J. D. Watson, G. A. Csáthy, and M. J. Manfra, *Phys. Rev. Appl.* **3**, 064004 (2015).
- [9] Y. J. Chung, K. A. Villegas Rosales, K. W. Baldwin, P. T. Madathil, K. W. West, M. Shayegan, and L. N. Pfeiffer, *Nat. Mater.* **20**, 632 (2021).
- [10] S. K. Singh, C. Wang, C. T. Tai, C. S. Calhoun, A. Gupta, K. W. Baldwin, L. N. Pfeiffer, and M. Shayegan, *arXiv:2309.00111*.
- [11] E. McCann and V. I. Fal'ko, *Phys. Rev. Lett.* **96**, 086805 (2006).
- [12] C. Dean, P. Kim, J. I. A. Li, and A. Young, in *Fractional Quantum Hall Effects: New Developments* (World Scientific, Singapore, 2020), pp. 317–375.
- [13] B. E. Feldman, J. Martin, and A. Yacoby, *Nat. Phys.* **5**, 889 (2009).
- [14] J. Martin, B. E. Feldman, R. T. Weitz, M. T. Allen, and A. Yacoby, *Phys. Rev. Lett.* **105**, 256806 (2010).
- [15] C. R. Dean, A. F. Young, I. Meric, C. Lee, L. Wang, S. Sorgenfrei, K. Watanabe, T. Taniguchi, P. Kim, K. L. Shepard, and J. Hone, *Nat. Nanotechnol.* **5**, 722 (2010).
- [16] K. Lee, B. Fallahazad, J. Xue, D. C. Dillen, K. Kim, T. Taniguchi, K. Watanabe, and E. Tutuc, *Science* **345**, 58 (2014).
- [17] A. Kou, B. E. Feldman, A. J. Levin, B. I. Halperin, K. Watanabe, T. Taniguchi, and A. Yacoby, *Science* **345**, 55 (2014).
- [18] D.-K. Ki, V. I. Fal'ko, D. A. Abanin, and A. F. Morpurgo, *Nano Lett.* **14**, 2135 (2014).
- [19] P. Maher, L. Wang, Y. Gao, C. Forsythe, T. Taniguchi, K. Watanabe, D. Abanin, Z. Papić, P. Cadden-Zimansky, J. Hone, P. Kim, and C. R. Dean, *Science* **345**, 61 (2014).
- [20] B. M. Hunt, J. I. A. Li, A. A. Zibrov, L. Wang, T. Taniguchi, K. Watanabe, J. Hone, C. R. Dean, M. Zaletel, R. C. Ashoori, and A. F. Young, *Nat. Commun.* **8**, 948 (2017).
- [21] K. Huang, H. Fu, D. R. Hickey, N. Alem, X. Lin, K. Watanabe, T. Taniguchi, and J. Zhu, *Phys. Rev. X* **12**, 031019 (2022).
- [22] A. A. Zibrov, C. Kometter, H. Zhou, E. M. Spanton, T. Taniguchi, K. Watanabe, M. P. Zaletel, and A. F. Young, *Nature (London)* **549**, 360 (2017).
- [23] J. I. A. Li, C. Tan, S. Chen, Y. Zeng, T. Taniguchi, K. Watanabe, J. Hone, and C. R. Dean, *Science* **358**, 648 (2017).
- [24] V. M. Apalkov and T. Chakraborty, *Phys. Rev. Lett.* **107**, 186803 (2011).
- [25] Z. Papić and D. A. Abanin, *Phys. Rev. Lett.* **112**, 046602 (2014).

- [26] A. C. Balram, *Phys. Rev. B* **105**, L121406 (2022).
- [27] H. Polshyn, H. Zhou, E. M. Spanton, T. Taniguchi, K. Watanabe, and A. F. Young, *Phys. Rev. Lett.* **121**, 226801 (2018).
- [28] Y. Zeng, J. I. A. Li, S. A. Dietrich, O. M. Ghosh, K. Watanabe, T. Taniguchi, J. Hone, and C. R. Dean, *Phys. Rev. Lett.* **122**, 137701 (2019).
- [29] J. P. Eisenstein, L. N. Pfeiffer, and K. W. West, *Phys. Rev. B* **50**, 1760 (1994).
- [30] F. Yang, A. A. Zibrov, R. Bai, T. Taniguchi, K. Watanabe, M. P. Zaletel, and A. F. Young, *Phys. Rev. Lett.* **126**, 156802 (2021).
- [31] P. L. Gammel, D. J. Bishop, J. P. Eisenstein, J. H. English, A. C. Gossard, R. Ruel, and H. L. Stormer, *Phys. Rev. B* **38**, 10128 (1988).
- [32] J. Falson, D. Maryenko, B. Friess, D. Zhang, Y. Kozuka, A. Tsukazaki, J. H. Smet, and M. Kawasaki, *Nat. Phys.* **11**, 347 (2015).
- [33] Q. Shi, E.-M. Shih, M. V. Gustafsson, D. A. Rhodes, B. Kim, K. Watanabe, T. Taniguchi, Z. Papić, J. Hone, and C. R. Dean, *Nat. Nanotechnol.* **15**, 569 (2020).
- [34] See Supplemental Material at <http://link.aps.org/supplemental/10.1103/PhysRevLett.132.046603> for additional data, experimental and theoretical details, which includes Refs. [35–38].
- [35] B. Huard, J. A. Sulpizio, N. Stander, K. Todd, B. Yang, and D. Goldhaber-Gordon, *Phys. Rev. Lett.* **98**, 236803 (2007).
- [36] R. Geick, C. H. Perry, and G. Rupprecht, *Phys. Rev.* **146**, 543 (1966).
- [37] T. Misumi and K. Shizuya, *Phys. Rev. B* **77**, 195423 (2008).
- [38] K. Maki and X. Zotos, *Phys. Rev. B* **28**, 4349 (1983).
- [39] J. K. Jain, *Phys. Rev. Lett.* **63**, 199 (1989).
- [40] M. Levin and B. I. Halperin, *Phys. Rev. B* **79**, 205301 (2009).
- [41] M. S. Bello, B. I. Shklovskii, E. I. Levin, and A. Efros, *Sov. Phys JETP* **53**, 822 (1981).
- [42] J. P. Eisenstein, L. N. Pfeiffer, and K. W. West, *Phys. Rev. Lett.* **68**, 674 (1992).
- [43] M. P. Zaletel, R. S. K. Mong, and F. Pollmann, *Phys. Rev. Lett.* **110**, 236801 (2013).
- [44] R. S. K. Mong, M. P. Zaletel, F. Pollmann, and Z. Papić, *Phys. Rev. B* **95**, 115136 (2017).
- [45] D. G. Polyakov and B. I. Shklovskii, *Phys. Rev. Lett.* **74**, 150 (1995).
- [46] N. d’Ambrumenil, B. I. Halperin, and R. H. Morf, *Phys. Rev. Lett.* **106**, 126804 (2011).
- [47] J. Nuebler, V. Umansky, R. Morf, M. Heiblum, K. von Klitzing, and J. Smet, *Phys. Rev. B* **81**, 035316 (2010).
- [48] Z. F. Ezawa and A. Iwazaki, *J. Phys. Soc. Jpn.* **61**, 4133 (1992).
- [49] K. K. W. Ma, M. R. Peterson, V. W. Scarola, and K. Yang, *Encycl. Condens. Matter Phys.* **1**, 324 (2024).
- [50] K. Shizuya, *Phys. Rev. B* **75**, 245417 (2007).
- [51] N. R. Cooper and A. Stern, *Phys. Rev. Lett.* **102**, 176807 (2009).
- [52] Y. Hu, Y.-C. Tsui, M. He, U. Kamber, T. Wang, A. S. Mohammadi, K. Watanabe, T. Taniguchi, Z. Papić, M. P. Zaletel, and A. Yazdani, [arXiv:2308.05789](https://arxiv.org/abs/2308.05789).